IL-4 downregulates BCL6 to promote memory B cell selection in germinal centers

Laila Shehata[1], Christopher D. Thouvenel[2], Brian D. Hondowicz[1], Lucia A. Pew[1], David J. Rawlings[1,2,3], Jinyong Choi[4], Marion Pepper[1*]

[1] Department of Immunology, University of Washington School of Medicine; Seattle, WA, USA.
[2] Center for Immunity and Immunotherapies, Seattle Children's Research Institute; Seattle, WA, USA.
[3] Department of Pediatrics, University of Washington School of Medicine; Seattle, WA, USA.
[4] Department of Microbiology, Department of Biomedicine & Health Sciences, College of Medicine, The Catholic University of Korea; Seoul, Korea.

* Corresponding author. Email: mpepper@uw.edu

Abstract
Germinal center (GC)-derived memory B cells (MBCs) are critical for humoral immunity as they differentiate into protective antibody-secreting cells during re-infection. GC formation and cellular interactions within the GC have been studied in detail, yet the exact signals that allow for the selection and exit of MBCs are not understood. We show that IL-4 can trigger GC B cell selection and exit by inducing the negative autoregulation of BCL6, the primary GC transcription factor. High affinity/avidity GC B cells that secure additional help and upregulate MBC survival signals to replace the loss of BCL6 exit the GC as memory cells, whereas those that do not are primed for cell death. In this way, IL-4 signaling regulates selection and affinity maturation within the MBC pool.

Introduction

Germinal centers (GCs) are highly organized structures found within B cell follicles. In the GC, activated B cells proliferate, diversify their B cell receptors, and are selected to mature into memory cells that provide humoral protection from disease (*1*). Temporally and spatially distinct and complex interactions between B cells and other cells in the GC including $CD4^+$ T follicular helper (Tfh) cells and follicular dendritic cells (FDCs) influence the initiation, maintenance, and dissolution of GCs. While many of these interactions have been well-characterized, many others, including how affinity-matured memory B cells (MBCs) are selected to exit the GC, remain poorly defined (*2–9*). Specifically, the mechanisms underlying the selection process that leads to the downregulation of GC-defining transcriptional programs and concomitant upregulation of transcriptional programs associated with long-lived memory B cell formation are unknown (*10–12*). It is well accepted that BCL6, a repressive transcription factor, actively maintains the GC and must be downregulated for MBCs to form, but the signals that initiate the downregulation of BCL6 have not been identified (*13*, *14*). Understanding how this process takes place is critical for generating high affinity memory B cell formation for optimal vaccine development or to target this process therapeutically during autoimmunity.

Interleukin-4 (IL-4) is a key T cell-derived molecule that has been attributed with conflicting roles in the regulation of the GC (*15*, *16*). Early after the initiation of an anti-viral response, IL-4 produced by natural killer T cells is able to stimulate GC formation by promoting B cell expression of BCL6 (*15*, *17*, *18*). BCL6 acts via repressor-of-repressor circuits to activate

transcriptional programs that keep B cells and Tfh cells tethered in the GC and prevent them from terminally differentiating (*14*, *19*, *20*). BCL6 also suppresses the DNA damage sensor ATR, thereby acting as an anti-apoptotic factor to keep GC B cells alive as they undergo rounds of DNA damage-prone somatic hypermutation (*21*, *22*). Yet how subsequent IL-4 production by $CD4^+$ Tfh and GC Tfh cells impacts BCL6 expression, GC maintenance, and memory formation is unclear. Very recent work from Duan and colleagues demonstrated that excess availability of IL-4 could reduce memory B cell formation, although the mechanism was not defined (*16*). Herein we have sought to define how IL-4 functions in the GC and to determine if it could influence the selection or exit of MBCs through its regulation of BCL6. We demonstrate that while IL-4 promotes BCL6 in naive B cells to encourage GC formation, it also induces the negative autoregulation of BCL6 in GC B cells. This IL-4-mediated downregulation of BCL6 initiates a selection event, allowing pre-memory GC B cells that can obtain additional survival signals to exit the GC, whereas those that cannot undergo cell death.

Results

IL-4 can be produced by GC Tfh cells and perceived by GC B cells during Plasmodium infection

To better understand how $CD4^+$ T cell-derived IL-4 can impact B cell differentiation during infection, we first characterized the identity and kinetics of IL-4-producing $CD4^+$ T cells specific for *Plasmodium*-derived antigens during an ongoing GC response. To accomplish this, KN2 (knock-in huCD2) mice that express cell surface-associated huCD2 protein under control of the IL-4 promoter were infected with 10^6 *Plasmodium yoelii*-GP66 (*P.y*-GP66)-infected red blood cells (iRBCs). We chose to examine IL-4 production from days 6-18 after *Plasmodium* infection as our previous work demonstrated that this is a critical window for *Plasmodium*-specific B cell differentiation, encompassing the initiation and propagation of the GC as well as early memory formation (*23*). IL-4 producing GP66-specific $CD4^+$ T cells were identified, analyzed, and enumerated using previously published tetramer enrichment and flow cytometric techniques (*24*). The early epitope-specific $CD44^+CD4^+$ T cell response to acute *Plasmodium* infection consists of a small population of $CXCR5^-$ T effector cells and a much larger population of $CXCR5^{int}PD1^{int}$ Tfh cells, with some of these cells continuing to differentiate into $CXCR5^{hi}PD1^{hi}$ GC Tfh cells as the response progresses (*24*). In response to *Plasmodium*, the number of IL-4-producing T cells increased throughout the acute stage of infection, as previously shown in influenza and helminth infections (*18*, *25*, *26*) (**Fig. 1, A, B, and C; fig. S1, A and B**). Of interest, although Tfh cells contributed to early IL-4 production, by day 8 the majority of IL-4-producing T cells were GC Tfh (66.8%), and this proportion steadily increased to 83% by day 18 (**Fig. 1, A, C, and D**). This indicates that in a Type 1 immune response to infection, the bulk of $CD4^+$ T cell-derived IL-4 is produced during an ongoing GC, suggesting contributions beyond solely early GC formation.

We also examined expression of the IL-4 receptor alpha chain (IL4Rα; CD124) on subsets of *Plasmodium*-specific B cells over the course of acute *P.y*-GP66 infection to determine their ability to respond to IL-4. We used a previously described strategy of magnetic bead enrichment of fluorophore-conjugated B cell tetramers that contained the *Plasmodium* blood-stage antigen Merozoite Surface Protein-1 (MSP1) to characterize IL4Rα expression on responding B cells (*23*). The MSP1-specific B cell response developed as previously described; a population of $CD138^+$ plasmablasts emerged early and peaked around 10 days post-infection, while $CD38^-GL7^+$ GC B cells expanded from approximately days 10-20 post-infection (*23*) (**Fig. 1E; fig. S1C**). MSP1-specific GC transit B cells were identified as $CD38^+GL7^+$ cells that consist of both activated cells entering the GC ($BCL6^+CD80^-$) or exiting the GC ($BCL6^-CD80^+$). GC transit B cells expanded as

GCs formed, but stabilized at day 15, whereas the $CD38^+GL7^-$ population consisting of memory and naive B cells increased steadily over the course of acute infection.

Examination of IL4Rα expression revealed a large population of $IL4R\alpha^+$ MSP1-specific $CD38^+GL7^-$ B cells in uninfected mice (day 0), suggesting naive B cells can receive IL-4 signals early in infection (**Fig. 1F; fig. S1D**). Very few plasmablasts expressed IL4Rα, consistent with prior work demonstrating that IL-4 may regulate B cell migration into B cell follicles and away from the extrafollicular regions where early plasmablasts form (*27*). However, all other B cell subsets – including GC B cells – highly expressed IL4Rα throughout acute infection (**Fig. 1G**). Overall, this demonstrates that B cells are capable of perceiving Tfh- and GC Tfh-derived IL-4 both prior to and within an ongoing GC.

IL-4 has opposing effects on the B cell response over the course of infection

The kinetics of $CD4^+$ GC Tfh production of IL-4 in conjunction with GC B cell expression of IL4Rα suggested a role for IL-4 in the GC that perhaps went beyond solely GC entry. We therefore asked how *in vivo* administration of exogenous IL-4 at a variety of time points affects GC B cell development after *Plasmodium* infection. We infected C57BL/6 (WT) mice with 10^6 *Plasmodium chabaudi* (*P.ch*)-iRBCs and administered IL-4 complexed to anti-IL-4 antibody (IL4C) or phosphate buffered saline (PBS) intravenously on the first 3 days of infection to determine if early IL-4 enhances GC formation as seen in other infections (*18*, *28*) (**Fig. 2A**). In accordance with prior results in influenza infection, we observed a significant increase in the number and frequency of MSP1-specific GC B cells by day 8 post-infection in mice treated with IL4C compared to untreated controls, suggesting that this role for early IL-4 in promoting GCs is universal (**Fig. 2, B, C, and D**).

We next asked if IL4C administration to *P.ch*-infected WT mice during an ongoing GC had a similar effect. Mice were administered PBS or IL4C in staggered three-day windows following GC formation (day 10) and the MSP1-specific B cell response was analyzed one day following the last treatment (**Fig. 2E**). Although there was no significant impact on the B cell response when mice received IL4C on days 10 and 12, there was a surprising loss of MSP1-specific B cells when IL4C was administered on days 12 and 14 (**Fig. 2, F and G**). A similar trend was observed for the later IL4C treatment windows as well. Importantly, MSP1-specific cells in IL4C-treated mice did not have higher BLIMP1 expression, plasmablast numbers, or anti-MSP1 serum IgG, indicating that IL-4 is not diverting B cells to a plasmablast fate (**fig. S2 A-G**). Thus, although early IL-4 encourages GC formation and ensuing antigen-specific GC B cell expansion, IL-4 restrains the B cell response once GCs have developed, in accordance with work by Duan and colleagues (*16*). Of interest, in mice treated with IL4C on days 12 and 14 that experienced the greatest loss of MSP1-specific B cells, there were surprisingly no significant changes in the frequencies of any one specific B cell subset (**Fig. 2H**), suggesting that IL-4 may be impacting and restricting the GC process, which could impact multiple subsets equally.

IL-4 downregulates BCL6 and enhances expression of CD80

To test if IL-4 was restricting the GC, we next imaged spleens to visualize GCs in mice treated with IL4C on days 12 and 14. Interestingly, we found that GCs in IL4C-treated mice were smaller in size, supporting the hypothesis that IL-4 can constrain an ongoing GC response (**fig. S3, A and B**). As GCs are highly regulated by BCL6, we also stained for BCL6 expression by flow cytometry after IL4C treatment. In opposition to the current paradigm that IL-4 promotes BCL6, we observed an insignificant decrease in BCL6 expression in GC B cells as well as a stark loss of

BCL6 in GC transit B cells in IL4C-treated mice compared to controls(**Fig. 3, A and B**). One possibility was that IL-4 signaling may differentially affect naive and GC B cells, which would reconcile the opposing B cell responses to IL-4 that we observed with early versus late IL4C treatments. We therefore isolated splenic B cells from *Plasmodium*-infected mice and cultured them in the presence or absence of IL-4 (10 ng/mL) for 24 hours. Phenotypically naive B cells ($B220^+IgD^+CD38^+GL7^-CD73^-CD80^-$) analyzed after 24h culture with IL-4 had significantly higher BCL6 expression than those cultured in media alone, consistent with previous literature (*17*) (**Fig. 3C**). However, $GL7^+$ B cells ($B220^+CD138^-IgD^-GL7^+$) analyzed after 24h culture in the presence of IL-4 lost BCL6 expression (**Fig. 3D**), mirroring the *in vivo* phenotype observed in mice treated with IL4C on days 12 and 14 (**Fig 3B**). This loss of BCL6 in response to IL-4 treatment *in vitro* cannot be attributed to an increased loss of $GL7^+$ B cells, as the numbers of total $GL7^+$ B cells recovered at 24h were similar between groups (**Fig. 3E**). This indicates that IL-4 can have opposing effects on B cell BCL6 expression, perhaps contingent on the level of BCL6 already present in the cell.

IL-21 and BLIMP1 are known to initiate the downregulation of BCL6 for plasma cell exit in late GCs, but the signals that initiate BCL6 downregulation for MBC exit are unknown (*29*, *30*). If IL-4 can induce GC B cell downregulation of BCL6 and release GC B cells from the repressive BCL6 transcriptional program, we hypothesized that those cells may also alter their phenotype and migrate out of the GC as long-lived MBCs (*31*). We therefore repeated the experiment, this time performing an analysis of IL-4-induced phenotypic changes related to memory formation. Specifically, co-expression of cell surface proteins CD73 and CD80 define memory B cells that are highly mutated and rapidly differentiate into antibody-secreting cells upon re-challenge (*23*, *32–34*). Of interest, CD80 expression is repressed by BCL6 and is therefore enhanced as GC B cells lose BCL6 expression and re-upregulate CD38 to form MBCs (*35*). Although there were fewer MSP1-specific GC transit B cells in IL4C-treated mice compared to controls, within that population there was a reduced frequency of $BCL6^+$ cells and a concomitant increase in the frequency of $CD80^+$ cells compared to GC transit cells in control mice (**Fig. 3F**). However, despite the proportional increase in GC-exiting $CD80^+$ B cells found in the $CD38^+GL7^+$ transiting population, IL4C-treated mice exhibited a specific loss of GC-derived class-switched (IgM^-IgD^-; $swIg^+$) $CD73^+CD80^+CD38^+GL7^-$ MBCs (**Fig. 3G; fig. S3C**). Thus, although IL-4 appears to be increasing GC exit into the transiting pool, the overall loss of MSP1-specific B cells and of GC-derived MBCs suggests that the IL-4-mediated loss of BCL6 may also be resulting in GC B and transit B cells dying instead of successfully forming long-lived memory.

IL-4 treatment results in BCL6 downregulation via the negative autoregulation of BCL6

To account for the surprising IL4C-mediated loss of BCL6 expression in $GL7^+$ B cells, we hypothesized that we had invoked the ability of BCL6 to negatively autoregulate and reduce its own expression levels, a process that is often disrupted in B cell lymphomas (*19*, *36*, *37*). It was formally possible that while early IL-4 enhances BCL6 expression and GC entry early in an immune response, administration of IL-4 to GC B cells that express a high enough threshold of BCL6 may promote BCL6 to bind its own promoter and negatively autoregulate. IL-4 acts through STAT6 to promote BCL6 expression via the STAT6 binding site in the BCL6 promoter region (*17*, *38*). Interestingly, phosphorylated STAT6 has also been shown to directly lead to the repression of BCL6 transcription in primary mediastinal B cell lymphomas (*39*). To demonstrate a role for STAT6 signaling in the IL-4-mediated repression of BCL6, we treated *P.ch*-infected WT and STAT6-deficient (STAT6KO) mice with IL4C and analyzed BCL6 and CD80 expression in

MSP1-specific GC transit B cells as above. Of interest, both GC B cells and GC transit B cells in both WT and STAT6KO mice were able to express equivalent amounts of BCL6, consistent with prior literature that IL-21 and other molecules contribute to B cell expression of BCL6 (*15*, *40*, *41*) (**Fig. 4, A and B**). However, while IL4C treatment of WT cells led to BCL6 downregulation and CD80 upregulation as demonstrated above, GC transit B cells that lack STAT6 did not alter their expression of BCL6 or CD80 in response to IL4C, demonstrating that this IL-4 driven process is STAT6-dependent (**Fig 4, B, and C**).

We then directly tested if the IL-4-STAT6 pathway was promoting BCL6 to a threshold that triggered its negative autoregulation by using ΔBPS1 mice, which have an 8-nucleotide deletion in the BCL6 promoter binding site 1 (BPS1) that prohibits BCL6 from binding to its own promoter (*19*). We adoptively transferred splenic B cells isolated from CD45.2$^+$ ΔBPS1 mice into CD45.1$^+$ WT hosts, infected the hosts with *P.ch* and treated the mice with IL4C on days 12 and 14, prior to analysis of the MSP1-specific B cell response on day 15 (**Fig. 4D; fig. S3D**). In both GC B cells and GC transit B cells, BCL6 expression remained significantly higher in the ΔBPS1 cells than in WT cells (**Fig. 4, E and F**). Additionally, the IL-4-mediated downregulation of BCL6 in WT GC transit B cells corresponded to an increase in CD80 expression, whereas CD80 was not upregulated in ΔBPS1 GC transit B cells after IL4C treatment (**Fig. 4G**). Together, these data show that IL-4 signaling via STAT6 leads to BCL6 negative autoregulation in GL7$^+$BCL6$^+$ B cells, increasing GC exit via a CD38$^+$GL7$^+$CD80$^+$ transition stage, yet these cells do not survive to become MBCs.

IL-4 treatment is not sufficient to upregulate MBC survival proteins

We next sought to determine whether the lack of expansion of swIg$^+$ MBCs following IL4C treatment was due in part to increased cell death of B cells that had downregulated BCL6 but did not upregulate a replacement survival signal. BCL6 has been shown to directly repress two such signals; the transcription factor c-myc and the protein BCL2 (*12*, *42*). A transient downregulation of BCL6 in the GC can correspond to a transient upregulation of c-myc, which protects from apoptosis by promoting cell cycle entry as GC B cells migrate to the dark zone to undergo clonal expansion (*11*). These positively selected cells can also be identified by their expression of the surface marker CD23, which is upregulated on GC B cells that have recently received IL-4 and/or CD40L signals from T cells (*16*, *42*). To determine if selection into the dark zone was impaired by IL4C treatment, we infected WT mice with *P.ch*, treated them with IL4C on days 12 and 14, and analyzed the expression of CD23 and c-myc in three distinct populations that appear to be directly impacted by IL-4 signaling: GC B cells, BCL6$^-$CD80$^+$ GC transit B cells (exiting GC), and CD73$^{and/or}$CD80$^+$ memory B cells (**Fig. 5A**). Importantly, IL4C treatment increased CD23 expression in all three populations, although most significantly in the BCL6$^-$CD80$^+$ GC transit B cells (**Fig. 5B; fig. S4A**). This is consistent with our hypothesis that all three populations are responding to IL-4, and that IL-4 is specifically promoting GC exit. However, IL4C treatment did not affect c-myc expression in any of the three populations, indicating that IL-4 does not impact GC cycling (**Fig. 5C; fig. S4B**).

BCL6 is also known to repress BCL2, an anti-apoptotic protein that is highly expressed by both naive and memory B cells, and is critical for MBC survival (*43*). To test if IL4C was impairing the ability of exiting GC B cells to upregulate BCL2, we repeated the experiment and analyzed the expression of BCL2 on the same three populations as above. Interestingly, both GC B cells and MBCs from mice treated with IL4C failed to upregulate BCL2 to the same extent as control-treated mice, while BCL2 expression in BCL6$^-$CD80$^+$ GC transit B cells was unchanged between groups

(**Fig. 5, D, E, and F**). Together, these data suggest that IL-4 downregulates BCL6 in GC B cells but is insufficient to upregulate BCL2 to replace BCL6 as an anti-apoptotic signal. This results in an increase in GC exit, but may also lead to cell death, as exiting GC B cells that lack both BCL6 and BCL2 would not have the signals needed to survive as long-lived MBCs.

BCL2 protects GC B cells from IL-4 mediated cell death

To test if diminished expression of BCL2 in GC B cells and MBCs following IL4C treatment is leading to increased death of pre-memory GC B cells and recently formed MBCs, we administered IL4C or PBS simultaneously with the pan-caspase inhibitor emricasan to WT mice infected with *P.ch* (**Fig. 6, A and B**). Emricasan treatment resulted in an increase in MSP1-specific B cells regardless of PBS or IL4C treatment, demonstrating that blocking cell death increases MSP1-specific B cell numbers in the presence or absence of IL-4 treatment as expected (**Fig. 6C**). However, while mice treated with both PBS and emricasan had only modest increases in GC B cells and swIg$^+$CD73$^+$CD80$^+$ MBCs compared to PBS-treated mice (fold changes of 1.22 and 0.15, respectively), mice receiving IL4C and emricasan had a 5-fold increase in GC B cells and a 6-fold increase in swIg$^+$CD73$^+$CD80$^+$ MBCs compared to mice treated with IL4C alone (**Fig. 6, D and E**; **fig. S5A**). Additionally, mice treated with IL4C and emricasan had a higher frequency BCL6$^-$ GC B cells compared to mice treated with PBS and emricasan, indicating that there is a larger proportion of GC B cells dying due to IL-4-mediated downregulation of BCL6 (**fig. S5B**).

To determine if constitutively-expressed BCL2 is sufficient to rescue GC and memory B cells from IL-4-induced cell death, we used BCL2 transgenic mice (BCL2-Tg), which have a functional human BCL2 transgene expressed only in the murine B cell lineage (*10*). We infected WT and BCL2-Tg littermates with *P.ch* and treated them with IL4C or PBS on days 12 and 14 (**Fig. 6, F and G**). On day 15, IL4C-treated BCL2-Tg mice had significantly expanded MSP1-specific B cells compared to IL4C-treated WT littermates, while there is only a slight increase between the PBS-treated groups (**Fig. 6H**). As BCL2 is antagonistic to the GC transcriptional program, BCL2-Tg mice did not have increased GC B cells but did have a significantly higher number of total MBCs (CD73$^{\text{and/or}}$CD80$^+$) with either treatment (**Fig. 6I; fig. S5C**). However, IL4C treatment in BCL2-Tg mice resulted in a significant increase in swIg$^+$CD73$^+$CD80$^+$ MBCs compared to littermate controls, whereas PBS treatment in BCL2-Tg mice did not specifically impact swIg$^+$CD73$^+$CD80$^+$ MBCs in the same way, indicating that IL-4 treatment is promoting the formation of GC-derived MBCs (**Fig. 6J**). Together, these data demonstrate that the loss of B cells in response to IL4C treatment is due to pre-memory swIg$^+$ GC B cells downregulating BCL6 without upregulating BCL2, resulting in cell death.

IL-4 selects MBCs in the GC

The process of GC B cell affinity maturation involves consecutive rounds of BCR somatic hypermutation (SHM) and affinity-driven selection via B cell interactions with antigen-retaining FDCs and CD4$^+$ T cells, as described by multiple models (*44*). We observed increased GC exit and B cell death following IL4C treatment, suggesting that at physiological levels, IL-4 can promote positive selection and MBC exit via the downregulation of BCL6 if paired with additional receptor/ligand signals. In our experimental model, the addition of IL4C may unbalance the system such that more GC B cells downregulate BCL6 than can receive these critical, additional survival signals, leading to a net loss of cells. We therefore sought to determine if in the presence of physiological levels of IL-4 signaling, an inability to perceive IL-4 could increase GC B cell

survival while still allowing MBCs to form, resulting in a more diverse, lower affinity pool of MBCs.

To test this, we infected WT mice and IL4Rα-deficient (IL4RαKO) with *P.y*-GP66 to determine the impact on MBC formation (*45*, *46*). Importantly, IL4RαKO mice have been shown to develop GCs at a similar rate to WT mice, likely due to the outsize role of IL-21 in promoting GC formation and in keeping with our data demonstrating equivalent BCL6 expression in STAT6KO B cells (*15*, *47*). We therefore analyzed the MSP1-specific B cell response 60 days post-infection, when any differences in MBC formation should be apparent (**Fig. 7A**). WT and IL4RαKO mice had similar numbers of total MSP1-specific B cells and MBCs, and no differences in the number of swIg$^+$CD73$^+$CD80$^+$ MBCs (**Fig. 7, B, C, D, and E**). However, IL4RαKO mice had significantly larger GCs at day 60 by both number and frequency (**Fig. 7F**). The larger GCs cannot be attributed to a lack of parasite clearance, as the IL4RαKO mice controlled parasitemia as well as the WT mice throughout infection (**fig. S6, A and B**). This demonstrates that IL-4 promotes GC exit, but is not required for MBC formation as MBCs can still form in the absence of IL-4 signaling. Likely due to the longer lasting GCs, we also observed that there were fewer MSP1-specific long-lived plasma cells (LLPCs) in the bone marrow of IL4RαKO mice compared to WT mice at day 60 (**fig. S6C**). However, there were no significant differences in serum anti-MSP1 IgG levels as measured by ELISA or by stringent ELISA, which gives a measure of antibody affinity/avidity through a urea wash that disrupts weaker bonds (**fig. S6, D and E**). Thus, while IL-4 may impact MBC survival and selection within the GC, it does not seem to affect plasma cell selection.

Next, we assessed whether the larger GCs late in infection in IL4RαKO mice were due to a loss of IL-4-mediated pre-MBC selection, which would also impact the repertoire of MBCs that were able to exit the GC. We sorted MSP1-specific CD73$^+$CD80$^+$ MBCs from WT and IL4RαKO mice 60 days post-infection and performed paired heavy and light chain sequencing of their B cell receptors (BCRs) to determine the variable heavy chain (V_H) gene usage (**fig. S6F**). Interestingly, within the swIg$^+$ MBC population, there were several shared V_H genes with unequally distributed gene representation and some unique gene usage seen only in the WT or IL4RαKO groups (**Fig. 7G; fig. S6G**). Together these data suggest that a lack of IL-4 signaling allows for increased GC B cell persistence, which impacts the resulting MBC repertoire and thus potentially the functionality of the MBC pool.

Memory B cells formed in the absence of IL-4 signaling do not expand in response to re-infection

To determine the physiological relevance of a longer lasting, less selective GC on the quality of the memory B cell pool, we re-challenged WT and IL4RαKO mice with 10^7 *P.y*-GP66-iRBCs at day 60 and analyzed the B cell and serum antibody response 5 days post-challenge, when MBCs have begun to differentiate into plasmablasts (*23*) (**Fig. 8A**). Interestingly, there were fewer total MSP1-specific B cells 5 days after re-challenge in the IL4RαKO mice compared to WT mice, despite similar numbers of antigen-specific memory B cells formed by day 60 in the two groups (**Fig. 7D; Fig. 8, B and C**). Re-challenged IL4RαKO mice displayed minimal MBC proliferation compared to WT mice, including a lack of expansion of swIg$^+$CD73$^+$CD80$^+$ MBCs (**Fig. 8, D and E; fig. S7, A, and B**). Serum anti-MSP1 IgG levels were similar between the two re-challenged groups, indicating a similar amount of antibody being produced by MBC-derived plasmablasts (**fig. S7C**). Stringent ELISAs, however, revealed a significant reduction in signal from day 5 in serum from IL4RαKO mice compared to serum from WT mice, suggesting that the bulk of

IL4RαKO MBC-derived antibodies were lower affinity than those from WT mice (**Fig. 8F**). Together, these data demonstrate that in the absence of IL-4 signaling, there is a loss of selection that allows lower affinity GC B cells to survive and persist into the memory pool, resulting in a weaker response to challenge.

Discussion

Our data support a model in which IL-4 can promote either GC B cell entry or exit depending on the amount of BCL6 expression in a given cell. IL-4 produced by NKT cells or Tfh cells early in an immune response can act on activated naive B cells to promote BCL6 expression and thereby promote migration into GCs (*17*, *18*, *27*). Several groups have identified that after this early stage of GC formation, there continues to be a significant amount of IL-4 produced within the GC itself (*48–50*), consistent with our own findings that GC Tfh are the dominant $CD4^+$ T cell source of IL-4 in a Type 1 infection. However, the role of IL-4 beyond GC formation has only recently been examined through work from Duan and colleagues (*16*), which demonstrated that IL-4 in the GC can constrain memory cell formation. In keeping with earlier reports that IL-4 is broadcast around a T cell instead of secreted directly at the synapse (*51*), their data suggested that IL4Rα expressed on FDCs serves as a sink for excess IL-4, thereby limiting its effects on bystander GC B cells that are not actively engaged with a GC Tfh cell.

Here, we demonstrate that both exogenous and endogenous levels of IL-4 act on GC B cells to downregulate BCL6, due to IL-4 promoting BCL6 expression to a threshold which triggers its own negative autoregulation (*19*, *36*, *37*). IL4C-mediated loss of BCL6 also corresponded to a lack of upregulation of BCL2, a protein necessary for MBC survival, resulting in increased GC and memory B cell death. Treating mice with IL4C without simultaneously increasing the amount of available antigen or antigen-specific GC Tfh cells would increase the number of GC B cells receiving IL-4 without additional signals required to either re-upregulate BCL6 for GC cycling or upregulating BCL2 for successful memory exit. The exact signals required for either of these outcomes are unknown, but previous studies have dissected how the strength of T cell-B cell receptor-ligand interactions can dictate whether a GC B cell migrates to the DZ or differentiates in to a memory B cell or plasma cell, thus the amount of IL-4 received may also factor into these fate choices (*2*, *5*, *34*, *52*). Similarly, IL-21 has been shown to play an important role in clonal expansion in the DZ as well as in long-lived plasma cell formation (*41*, *53–55*). What makes a Tfh cell secrete IL-4 versus IL-21 in response to an interaction with a GC B cell has not been determined, however it is known that very few Tfh cells can produce both cytokines simultaneously (*26*). IL-4 and IL-21 production appear to be relatively segregated to the light zone or dark zone, respectively (*15*, *26*, *50*), suggesting cytokine signals in the GC may be temporally and spatially regulated, and perhaps memory B cell versus plasma cell fate are as well.

A crucial consequence of GC B cell death following IL-4-mediated downregulation of BCL6 is the link between cell death and selection in the GC. We found that in the absence of IL4Rα signaling, *Plasmodium*-infected mice had longer lasting GCs and distinct MBC V_H gene usage, suggesting a potential lack of positive selection that would limit survival to high affinity clones over their lower affinity counterparts. Indeed, in response to re-challenge, MBCs that formed in IL4RαKO mice did not proliferate as well as WT MBCs and differentiated into lower affinity antibody-secreting cells. Although other T cell signals such as CD40 can transiently downregulate BCL6 (*56*), this demonstrates that the lack of IL-4-mediated BCL6 downregulation results in less selection in IL4RαKO mice.

The signals underlying GC B cell selection and memory B cell exit have remained elusive, in part due to the complex nature of cellular interactions in the GC. The finding that IL-4 can promote GC entry early in an immune response as well as initiate selection and exit later in the GC illuminates a significant role for this cytokine that is distinct from its function in Type 2 immune responses. How GC B cells integrate IL-4 with other cytokine or receptor-ligand signals remains to be determined, yet the ability to modulate IL-4 throughout an immune response may on its own allow for the manipulation of MBC affinity in vaccine settings.

Materials and Methods

Mice

C57BL/6, CD45.1^{+} (B6.SJL-*Ptprc*^{a} *Pepc*^{b}*/BoyJ*) and STAT6KO (B6.129S2(C)-*Stat6*^{tm1Gru}/J) (*57*) mice were purchased from Jackson laboratories. IL4RαKO (IL-4Rα$^{-/-}$) mice (*58*) were provided by Dr. Frank Brombacher and were bred and maintained in our laboratory. KN2$^{+/+}$ mice were provided by Dr. Markus Mohrs (*59*). This strain was crossed to C56BL/6 mice to generate KN2$^{+/-}$ mice. ΔBPS1 mice were provided by Dr. Jinyong Choi (*19*). BCL2-Tg (B6.Cg-Tg(BCL2)22Wehi/J) mice were provided by Dr. Chris Allen (*60*). All mice were bred and housed under specific-pathogen free conditions at the University of Washington. All experiments were performed in accordance with the University of Washington Institutional Care and Use Committee guidelines.

Infections and parasitemia analysis

Plasmodium chabaudi chabaudi (AS) parasites and *Plasmodium yoelii 17XNL-GP66* parasites were maintained as frozen blood stocks and passaged through donor mice. Primary mouse infections were initiated by intraperitoneal (i.p.) injection of 10^{6} infected red blood cells (iRBCs) from donor mice. Re-challenge experiments were performed by injecting mice with 10^{7} iRBCs i.p. 60 days after primary injection. Parasitemia was measured by flow cytometry by fixing a drop of blood with 0.025% glutaraldehyde, then staining with CD45 APC (Clone 30-F11, BD Biosciences), Ter119 FITC (BD Biosciences), CD71 PE (Clone R17217, Invitrogen), and Hoechst33342.

Tetramers

The GP66$_{-77}$:I-A^{b}-APC tetramer (I-A^{b}/LCMV.GP66.DIYKGVYQFKSV) used for isolating GP66-specific T cells was obtained from the National Institutes of Health Tetramer Core. For *P.ch* MSP1-specific B cell isolation, recombinant His-tagged C-terminal MSP1 protein (amino acids 4960 to 5301) from *P.ch* was produced by *Pichia pastoris* and purified using a Ni-NTA agarose column as previously described (*61*). For *P.y*-GP66 MSP1-specific B cell isolation, a plasmid containing His-tagged 14 kD truncated carboxy terminus of *P.y* MSP1 protein (amino acids 1662-1757) was transfected into HEK293F cells and purified using a Ni-NTA agarose column as described previously (*62*). Purified *P.ch* MSP1 protein and purified *P.y* MSP1 protein were biotinylated using the EZ-Link Sulfo-NHS-LC Biotinylation Kit (ThermoFisher) and tetramerized with streptavidin-PE (Agilent) or streptavidin-APC (Agilent) as previously described (*23*, *63*). The PE decoy reagent to gate out non-MSP1-specific B cells was generated by conjugating SA-PE to AF647 using an AF647 antibody labeling kit (ThermoFisher Scientific), washing and removing any unbound AF647, and incubating with an excess of irrelevant biotinylated HIS-tagged protein. The APC decoy reagent was generated in the same manner, by conjugating SA-APC to Dylight 755 using a DyLight 755 antibody labeling kit (ThermoFisher Scientific).

Injections

For the administration of complexed IL-4 (IL4C), 5 ug of recombinant mouse IL-4 (BioLegend) was incubated with 25 ug of anti-mouse IL-4 antibody (11B11; BioXCell) for 2 minutes at room temperature (RT). The IL4C was then diluted to 150 uL with sterile PBS and administered intravenously (i.v.). Emricasan (Sigma-Aldrich) was resuspended to 2mg/mL in DMSO, prepared at 2.5 mg/kg in pre-warmed sterile PBS, and injected i.p.

Mouse cell enrichment and flow cytometry

Splenic cell suspensions were prepared and filtered through 100 uM Nitex mesh (Amazon). For B cell enrichment, cells were resuspended in 200 uL PBS containing 2% FBS and Fc block (2.4G2) and incubated with decoy tetramer at a concentration of 10 nM for 10 min at RT. MSP1-PE or -APC tetramer was added at a concentration of 10 nM and cells were incubated for 20 min on ice. Cells were washed, incubated with anti-PE or anti-APC magnetic beads (Miltenyi) for 30 min on ice, and passed over magnetized LS columns (Miltenyi) to elute the bound cells as previously described (*63*). For T cell enrichment, cells were resuspended in 200uL PBS containing 2% FBS and incubated with 10 nM GP66-77:I-A^b-APC tetramer for 1 hour at RT. Cells were washed, incubated with anti-APC magnetic beads, and passed over magnetized LS columns. All bound cells were stained with surface antibodies followed by fixation and intracellular antibody staining when needed (**table S1**). Cell counts were determined using Accucheck cell counting beads. Cells were analyzed on the Cytek Aurora and analyzed using FlowJo 10 software (Treestar).

In vitro splenocyte cultures

Splenic cell suspensions were prepared and filtered through 100 uM Nitex mesh. For negative selection of B cells, splenocytes were resuspended in 200 uL PBS containing 2% FBS and Fc block and incubated with biotin anti-mouse F4/80 (Clone BM8, BioLegend), CD3 (Clone 500A2, BD Biosciences), CD4 (Clone RM4-5, eBioscience), CD8 (Clone 53-6.7, eBioscience), and CD138 (Clone 281-2, BD Biosciences) for 20 min on ice. Cells were washed, incubated with anti-biotin magnetic beads (Miltenyi) for 30 min on ice, and passed over magnetized LS columns. Flow through was collected and 2 million B cells/well were added to 24-well plates in 2 mL DMEM (Gibco) supplemented with 10% FBS (R&D Systems), 1% penicillin/streptomycin (ThermoFisher Scientific), 15 mM Hepes (Gibco), and 55 uM β-mercaptoethanol (Gibco). 10 ng/mL of recombinant mouse IL-4 (BioLegend) diluted in PBS was added to wells cultured with the cytokine. Plates were incubated at 37ºC in a 5% CO2 incubator for 24h, then cells were harvested and washed with PBS containing 2% FBS and stained for flow cytometry as described above.

Adoptive cell transfers

Single cell suspensions from ΔBPS1 spleens were prepared and filtered through 100uM Nitex mesh. Red blood cells were lysed with ACK buffer (ThermoFisher Scientific). Naive B cells were isolated by negative magnetic activated cell sorting using the EasySep™ Mouse B cell Isolation Kit (StemCell Technologies). 30 million B cells were injected i.p. into $CD45.1^+$ mice.

ELISAs

96-well plates (Corning) were coated with 2 ug/mL of recombinant *P.ch* or *P.y* MSP1 diluted in PBS and incubated at 4°C overnight. Plates were washed with PBS containing 0.05% Tween-20 (PBS-T) and incubated with blocking buffer (PBS-T and 3% milk) for 1 hour at RT. Serum was

serially diluted in dilution buffer (PBS-T and 1% milk), added to plates, and incubated at RT for 2 hours. Plates were washed and incubated with biotin anti-mouse IgG (BioLegend) for 1 hour at RT, followed by Streptavidin-HRP (BD) for 30 min at RT. Bound antibodies were detected with 1X TMB (Invitrogen) and quenched with 1M HCl. Sample optical density (OD) was measured at 450 nM and 570 nM using an iMark Microplate Reader (Bio-Rad).

ELISpots

96-well ELISpot plates (Millipore) were coated with 20 ug/mL of recombinant *P.y* MSP1 diluted in PBS and incubated at 4°C overnight. Plates were washed with PBS-T and blocked with 1% BSA and 5% sucrose in PBS for 2h at RT. Single cell suspensions of murine bone marrow were prepared and passed over 100 uM Nitex mesh. Following red blood cell lysis, cells were plated onto coated ELIspot plates and incubated at 37°C for 5h. Cells were washed off and antibody secreting cells were detected using IgG biotin (BioLegend) followed by streptavidin-alkalkine phosphatase (R&D Systems). Spots were developed using BCIP/NBT (Mabtech) and were counted and analyzed using the CTL ELIspot reader and Immunospot analysis software (Cellular Technology Limited). Non-specific and background spots were determined by wells containing no cells. The number of spots detected per well was used to calculate the spot frequency per 10,000 cells.

B cell sorting and BCR sequencing

Cells were processed and stained as described above, and sorted on a FACS Aria II cell sorter (BD) into SMART-Seq lysis buffer (Takara). cDNA was generated for each sample using the SMART-Seq v4 kit (Takara). Samples were end-repaired, A-tailed, and ligated with custom UMI adapters (IDT) (**table S2**) at 2 uM according to NEBNext Ultra II instructions (NEB). Libraries were prepped following NEBNext Immune Sequencing Kit's protocol (NEB), and qPCR was used to determine cycling conditions prior to plateau. Samples were pooled at equimolar concentration and ran on a MiSeq (Illumina) with a MiSeq Reagent Kit v3 (600-cycle) (Illumina).

BCR sequence processing

All samples were processed with an in-house pipeline using pRESTO, BBDuk, and custom python scripts (*64*, *65*). Sequences were filtered for Q20 average quality and the TSO sequence. Consensus sequences were made using the UMI, and leader sequences were removed. Paired ends were assembled and sequences with bases below Q30 were removed. Sequences were collapsed to remove duplicates and all sequences filtered for at least 2 reads. Resulting fastq files were submitted to IMGT for alignment. Clones were identified using Shazam and Change-O with a clustering threshold of 0.06 and 0.04 for day 60 and day 15 samples, respectively (*66*). Sequences were analyzed further in R (4.0.4) using tidyverse (1.3.0) (*67*).

Histology and image analysis

Spleens were isolated from infected mice and immediately submerged in BD Cytofix diluted 1:3 with PBS for 24h at 4°C. Spleens were then washed with PBS and dehydrated in 30% sucrose for 24h at 4°C before being embedded in OCT freezing medium. 18 uM sections were cut on a crysostat and stained with anti-mouse IgD ef450 (Clone 11-26c, Invitrogen), CD3 AF488 (Clone 17A2, BioLegend), BCL6 AF647 (Clone K112-91, BD Biosciences), and CD35 biotin (Clone 8C12, BD Biosciences), followed by Streptavidin Cy3 (Jackson ImmunoResearch). Slides were cover-slipped with Fluoromount G mounting media (SouthernBiotech) and images were acquired

on a Nikon Eclipse 90i with NIS-Elements software. Imaris (Bitplane) was used for image analysis. GC diameter and circumference were measured as the area around or across the $BCL6^+$ cells using Imaris, with each measurement taken three times and averaged.

Statistical analysis

All statistical analyses were performed in GraphPad Prism 9 (GraphPad Software). Unpaired, two-tailed Student's t tests were applied to determine the differences between two individual groups. Paired, two-tailed Student's t tests were applied to determine the differences between two groups in adoptive transfer experiments. In the event of three or four groups, a one-way ANOVA followed by Tukey's multiple comparisons test was performed. The statistical details of each experiment are indicated in the figure legends.

References and Notes:

1. L. Mesin, J. Ersching, G. D. Victora, Germinal Center B Cell Dynamics. *Immunity*. **45** (2016), pp. 471–482.
2. W. Ise, K. Fujii, K. Shiroguchi, A. Ito, K. Kometani, K. Takeda, E. Kawakami, K. Yamashita, K. Suzuki, T. Okada, T. Kurosaki, T Follicular Helper Cell-Germinal Center B Cell Interaction Strength Regulates Entry into Plasma Cell or Recycling Germinal Center Cell Fate. *Immunity*. **48**, 702-715.e4 (2018).
3. T. Inoue, I. Moran, R. Shinnakasu, T. G. Phan, T. Kurosaki, Generation of memory B cells and their reactivation. *Immunol Rev.* **283**, 138–149 (2018).
4. T. Inoue, R. Shinnakasu, C. Kawai, W. Ise, E. Kawakami, N. Sax, T. Oki, T. Kitamura, K. Yamashita, H. Fukuyama, T. Kurosaki, Exit from germinal center to become quiescent memory B cells depends on metabolic reprograming and provision of a survival signal. *J Exp Med*. **218** (2021), doi:10.1084/jem.20200866.
5. R. Shinnakasu, T. Inoue, K. Kometani, S. Moriyama, Y. Adachi, M. Nakayama, Y. Takahashi, H. Fukuyama, T. Okada, T. Kurosaki, Regulated selection of germinal-center cells into the memory B cell compartment. *Nat Immunol*. **17**, 861–869 (2016).
6. A. M. Haberman, D. G. Gonzalez, P. Wong, T. Zhang, S. M. Kerfoot, Germinal center B cell initiation, GC maturation, and the coevolution of its stromal cell niches. *Immunol Rev*. **288**, 10–27 (2019).
7. K. Ochiai, M. Maienschein-Cline, G. Simonetti, J. Chen, R. Rosenthal, R. Brink, A. S. Chong, U. Klein, A. R. Dinner, H. Singh, R. Sciammas, Transcriptional Regulation of Germinal Center B and Plasma Cell Fates by Dynamical Control of IRF4. *Immunity*. **38**, 918–929 (2013).
8. C. H. Yeh, T. Nojima, M. Kuraoka, G. Kelsoe, Germinal center entry not selection of B cells is controlled by peptide-MHCII complex density. *Nat Commun*. **9** (2018), doi:10.1038/S41467-018-03382-X.
9. J. T. Jacobsen, W. Hu, T. B. R. Castro, S. Solem, A. Galante, Z. Lin, S. J. Allon, L. Mesin, A. M. Bilate, A. Schiepers, A. K. Shalek, A. Y. Rudensky, G. D. Victora, Expression of Foxp3 by T follicular helper cells in end-stage germinal centers. *Science*. **373** (2021), doi:10.1126/SCIENCE.ABE5146.
10. K. G. C. Smith, U. Weiss, K. Rajewsky, G. J. V. Nossal, D. M. Tarlinton, Bcl-2 increases memory B cell recruitment but does not perturb selection in germinal centers. *Immunity*. **1**, 803–813 (1994).

11. D. Dominguez-Sola, G. D. Victora, C. Y. Ying, R. T. Phan, M. Saito, M. C. Nussenzweig, R. Dalla-Favera, The proto-oncogene MYC is required for selection in the germinal center and cyclic reentry. *Nat Immunol*. **13**, 1083–1091 (2012).
12. B. J. Laidlaw, L. Duan, Y. Xu, S. E. Vazquez, J. G. Cyster, The transcription factor Hhex cooperates with the corepressor Tle3 to promote memory B cell development. *Nat Immunol*. **21**, 1082–1093 (2020).
13. M. Saito, J. Gao, K. Basso, Y. Kitagawa, P. M. Smith, G. Bhagat, A. Pernis, L. Pasqualucci, R. Dalla-Favera, A Signaling Pathway Mediating Downregulation of BCL6 in Germinal Center B Cells Is Blocked by BCL6 Gene Alterations in B Cell Lymphoma. *Cancer Cell*. **12**, 280–292 (2007).
14. T. C. Kuo, A. L. Shaffer, J. Haddad, S. C. Yong, L. M. Staudt, K. Calame, Repression of BCL-6 is required for the formation of human memory B cells in vitro. *J Exp Med*. **204**, 819 (2007).
15. D. G. Gonzalez, C. M. Cote, J. R. Patel, C. B. Smith, Y. Zhang, K. M. Nickerson, T. Zhang, S. M. Kerfoot, A. M. Haberman, Nonredundant Roles of IL-21 and IL-4 in the Phased Initiation of Germinal Center B Cells and Subsequent Self-Renewal Transitions. *The Journal of Immunology*. **201**, 3569–3579 (2018).
16. L. Duan, D. Liu, J. An, B. J. Laidlaw, J. G. C. Correspondence, H. Chen, M. A. Mintz, M. Y. Chou, D. I. Kotov, Y. Xu, J. G. Cyster, Follicular dendritic cells restrict interleukin-4 availability in germinal centers and foster memory B cell generation. *Immunity*. **54** (2021), doi:10.1016/j.immuni.2021.08.028.
17. S. Chevrier, T. Kratina, D. Emslie, D. M. Tarlinton, L. M. Corcoran, IL4 and IL21 cooperate to induce the high Bcl6 protein level required for germinal center formation. *Immunol Cell Biol*. **95**, 925–932 (2017).
18. M. Gaya, P. Barral, M. Burbage, S. Aggarwal, B. Montaner, A. Warren Navia, M. Aid, C. Tsui, P. Maldonado, U. Nair, K. Ghneim, P. G. Fallon, R.-P. Sekaly, D. H. Barouch, A. K. Shalek, A. Bruckbauer, J. Strid, F. D. Batista, Initiation of Antiviral B Cell Immunity Relies on Innate Signals from Spatially Positioned NKT Cells. *Cell*. **172**, 517-533.e20 (2018).
19. J. Choi, H. Diao, C. E. Faliti, J. Truong, M. Rossi, S. Bélanger, B. Yu, A. W. Goldrath, M. E. Pipkin, S. Crotty, Bcl-6 is the nexus transcription factor of T follicular helper cells via repressor-of-repressor circuits. *Nat Immunol*. **21**, 777–789 (2020).
20. W. Ci, J. M. Polo, L. Cerchietti, R. Shaknovich, L. Wang, N. Y. Shao, K. Ye, P. Farinha, D. E. Horsman, R. D. Gascoyne, O. Elemento, A. Melnick, The BCL6 transcriptional program features repression of multiple oncogenes in primary B cells and is deregulated in DLBCL. *Blood*. **113**, 5536–5548 (2009).
21. T. Kumagai, T. Miki, M. Kikuchi, T. Fukuda, N. Miyasaka, R. Kamiyama, S. Hirosawa, The proto-oncogene Bcl6 inhibits apoptotic cell death in differentiation-induced mouse myogenic cells. *Oncogene*. **18**, 467–475 (1999).
22. S. M. Ranuncolo, J. M. Polo, J. Dierov, M. Singer, T. Kuo, J. Greally, R. Green, M. Carroll, A. Melnick, Bcl-6 mediates the germinal center B cell phenotype and lymphomagenesis through transcriptional repression of the DNA-damage sensor ATR. *Nat Immunol*. **8**, 705–714 (2007).
23. A. T. Krishnamurty, C. D. Thouvenel, S. Portugal, G. J. Keitany, K. S. Kim, A. Holder, P. D. Crompton, D. J. Rawlings, M. Pepper, Somatically Hypermutated Plasmodium-

Specific IgM(+) Memory B Cells Are Rapid, Plastic, Early Responders upon Malaria Rechallenge. *Immunity*. **45**, 402–14 (2016).
24. E. N. Arroyo, M. Pepper, B cells are sufficient to prime the dominant CD4+ Tfh response to Plasmodium infection. *Journal of Experimental Medicine*. **217** (2020), doi:10.1084/JEM.20190849.
25. J. Langhorne, S. Gillard, B. Simon, S. Slade, K. Eichmann, Frequencies of CD4+ T cells reactive with plasmodium chabaudi chabaudi: Distinct response kinetics for cells with Th1 and Th2 characteristics during infection. *Int Immunol*. **1**, 416–424 (1989).
26. J. S. Weinstein, E. I. Herman, B. Lainez, P. Licona-Limón, E. Esplugues, R. Flavell, J. Craft, TFH cells progressively differentiate to regulate the germinal center response. *Nat Immunol*. **17**, 1197–1205 (2016).
27. A. Turqueti-Neves, M. Otte, O. P. da Costa, U. E. Höpken, M. Lipp, T. Buch, D. Voehringer, B-cell-intrinsic STAT6 signaling controls germinal center formation. *Eur J Immunol*. **44**, 2130–2138 (2014).
28. I. M. Katona, C. R. Maliszewski F D Finkelman, K. B. Madden, S. C. Morris, J. M. Holmes, "cytokine-anti-cytokine antibody complexes. cytokines by injection of Prolongation of in vivo effects of exogenous Anti-cytokine antibodies as carrier proteins" (2021), (available at http://www.jimmunol.org/content/151/3/1235).
29. S. A. Diehl, H. Schmidlin, M. Nagasawa, S. D. van Haren, M. J. Kwakkenbos, E. Yasuda, T. Beaumont, F. A. Scheeren, H. Spits, STAT3-Mediated Up-Regulation of BLIMP1 Is Coordinated with BCL6 Down-Regulation to Control Human Plasma Cell Differentiation. *J Immunol*. **180**, 4805 (2008).
30. A. L. Shaffer, X. Yu, Y. He, J. Boldrick, E. P. Chan, L. M. Staudt, BCL-6 represses genes that function in lymphocyte differentiation, inflammation, and cell cycle control. *Immunity*. **13**, 199–212 (2000).
31. G. Cattoretti, R. Shaknovich, P. M. Smith, H.-M. Jäck, V. v. Murty, B. Alobeid, Stages of Germinal Center Transit Are Defined by B Cell Transcription Factor Coexpression and Relative Abundance. *The Journal of Immunology*. **177**, 6930–6939 (2006).
32. M. M. Tomayko, N. C. Steinel, S. M. Anderson, M. J. Shlomchik, Cutting Edge: Hierarchy of Maturity of Murine Memory B Cell Subsets. *The Journal of Immunology*. **185**, 7146–7150 (2010).
33. G. v. Zuccarino-Catania, S. Sadanand, F. J. Weisel, M. M. Tomayko, H. Meng, S. H. Kleinstein, K. L. Good-Jacobson, M. J. Shlomchik, CD80 and PD-L2 define functionally distinct memory B cell subsets that are independent of antibody isotype. *Nature Immunology 2014 15:7*. **15**, 631–637 (2014).
34. K. L. Good-Jacobson, E. Song, S. Anderson, A. H. Sharpe, M. J. Shlomchik, CD80 Expression on B Cells Regulates Murine T Follicular Helper Development, Germinal Center B Cell Survival, and Plasma Cell Generation. *The Journal of Immunology*. **188**, 4217–4225 (2012).
35. H. Niu, G. Cattoretti, R. Dalla-Favera, BCL6 controls the expression of the B7-1/CD80 costimulatory receptor in germinal center B cells. *Journal of Experimental Medicine*. **198**, 211–221 (2003).
36. L. Pasqualucci, A. Migliazza, K. Basso, J. Houldsworth, R. S. K. Chaganti, R. Dalla-Favera, Mutations of the BCL6 proto-oncogene disrupt its negative autoregulation in diffuse large B-cell lymphoma. *Blood*. **101**, 2914–2923 (2003).

37. L. M. Mendez, J. M. Polo, J. J. Yu, M. Krupski, B. B. Ding, A. Melnick, B. H. Ye, CtBP Is an Essential Corepressor for BCL6 Autoregulation. *Mol Cell Biol*. **28**, 2175–2186 (2008).
38. A. J. Schroder, P. Pavlidis, A. Arimura, D. Capece, P. B. Rothman, Cutting Edge: STAT6 Serves as a Positive and Negative Regulator of Gene Expression in IL-4-Stimulated B Lymphocytes. *The Journal of Immunology*. **168**, 996–1000 (2002).
39. O. Ritz, K. Rommel, K. Dorsch, E. Kelsch, J. Melzner, M. Buck, K. Leroy, V. Papadopoulou, S. Wagner, R. Marienfeld, S. Brüderlein, J. K. Lennerz, P. Möller, STAT6-mediated BCL6 repression in primary mediastinal B-cell lymphoma (PMBL). *Oncotarget*. **4**, 1093–1102 (2013).
40. M. A. Linterman, L. Beaton, D. Yu, R. R. Ramiscal, M. Srivastava, J. J. Hogan, N. K. Verma, M. J. Smyth, R. J. Rigby, C. G. Vinuesa, IL-21 acts directly on B cells to regulate Bcl-6 expression and germinal center responses. *Journal of Experimental Medicine*. **207**, 353–363 (2010).
41. D. Zotos, J. M. Coquet, Y. Zhang, A. Light, K. D'Costa, A. Kallies, L. M. Corcoran, D. I. Godfrey, K.-M. Toellner, M. J. Smyth, S. L. Nutt, D. M. Tarlinton, IL-21 regulates germinal center B cell differentiation and proliferation through a B cell-intrinsic mechanism. *J Exp Med*. **207**, 365–78 (2010).
42. R. Nakagawa, A. Toboso-Navasa, M. Schips, G. Young, L. Bhaw-Rosun, M. Llorian-Sopena, P. Chakravarty, A. K. Sesay, G. Kassiotis, M. Meyer-Hermann, D. P. Calado, Permissive selection followed by affinity-based proliferation of GC light zone B cells dictates cell fate and ensures clonal breadth. *Proceedings of the National Academy of Sciences*. **118** (2021), doi:10.1073/PNAS.2016425118.
43. K. G. C. Smith, A. Light, L. A. O'Reilly, S. M. Ang, A. Strasser, D. Tarlinton, bcl-2 Transgene expression inhibits apoptosis in the germinal center and reveals differences in the selection of memory B cells and bone marrow antibody-forming cells. *Journal of Experimental Medicine*. **191**, 475–484 (2000).
44. G. D. Victora, M. C. Nussenzweig, Germinal Centers. *https://doi.org/10.1146/annurev-immunol-120419-022408*. **40**, 413–442 (2022).
45. M. Parra, J. Yang, M. Weitner, S. Derrick, A. Yang, T. Schmidt, B. Singh, A. Moreno, M. Akkoyunlu, TACI contributes to plasmodium yoelii host resistance by controlling t follicular helper cell response and germinal center formation. *Front Immunol*. **9**, 2612 (2018).
46. Y. Fu, Y. Ding, T. Zhou, X. Fu, W. Xu, Plasmodium yoelii blood-stage primes macrophage-mediated innate immune response through modulation of toll-like receptor signalling. *Malar J*. **11**, 1–8 (2012).
47. M. Kopr, G. Kobler, J. Langhorne, "Max·Planck·lnstitut fiir Immunbiologie, Freiburg P. chabaudi infection in ll..-4-deficient mice The immune response to Plasmodium chabaudi malaria in interleukin-4-deficient mice*" (1994).
48. I. Yusuf, R. Kageyama, L. Monticelli, R. J. Johnston, D. DiToro, K. Hansen, B. Barnett, S. Crotty, Germinal Center T Follicular Helper Cell IL-4 Production Is Dependent on Signaling Lymphocytic Activation Molecule Receptor (CD150). *The Journal of Immunology*. **185**, 190–202 (2010).
49. I. L. King, M. Mohrs, IL-4-producing CD4+ T cells in reactive lymph nodes during helminth infection are T follicular helper cells. *Journal of Experimental Medicine*. **206**, 1001–1007 (2009).

50. R. L. Reinhardt, H.-E. Liang, R. M. Locksley, Cytokine-secreting follicular T cells shape the antibody repertoire. *Nat Immunol*. **10**, 385–393 (2009).
51. M. Huse, B. F. Lillemeier, M. S. Kuhns, D. S. Chen, M. M. Davis, T cells use two directionally distinct pathways for cytokine secretion. *Nature Immunology 2006 7:3*. **7**, 247–255 (2006).
52. T. Koike, K. Harada, S. Horiuchi, D. Kitamura, The quantity of CD40 signaling determines the differentiation of b cells into functionally distinct memory cell subsets. *Elife*. **8** (2019), doi:10.7554/eLife.44245.001.
53. C. Chou, D. J. Verbaro, E. Tonc, M. Holmgren, M. Cella, M. Colonna, D. Bhattacharya, T. Egawa, The Transcription Factor AP4 Mediates Resolution of Chronic Viral Infection through Amplification of Germinal Center B Cell Responses. *Immunity*. **45**, 570–582 (2016).
54. I. Quast, A. R. Dvorscek, C. Pattaroni, T. M. Steiner, C. I. McKenzie, C. Pitt, K. O'Donnell, Z. Ding, D. L. Hill, R. Brink, M. J. Robinson, D. Zotos, D. M. Tarlinton, Interleukin-21, acting beyond the immunological synapse, independently controls T follicular helper and germinal center B cells. *Immunity*. **0** (2022), doi:10.1016/J.IMMUNI.2022.06.020.
55. H. C. M. Iii, P. E. Lipsky, W. J. Leonard, D. J. Shaffer, S. Akilesh, D. C. Roopenian, H.-P. Kim, G. Wang, C.-F. Qi, P. K. Ozaki, R. Spolski, R. Ettinger, Inducer of Blimp-1 and Bcl-6 Plasma Cell Generation by IL-21, a Novel Regulation of B Cell Differentiation and. *J Immunol*. **173**, 5361–5371 (2021).
56. J. M. Polo, W. Ci, J. D. Licht, A. Melnick, Reversible disruption of BCL6 repression complexes by CD40 signaling in normal and malignant B cells. *Blood*. **112**, 644–651 (2008).
57. M. H. Kaplan, U. Schindler, S. T. Smiley, M. J. Grusby, Stat6 is required for mediating responses to IL-4 and for the development of Th2 cells. *Immunity*. **4**, 313–319 (1996).
58. M. Barner, M. Mohrs, F. Brombacher, M. Kopf, Differences between IL-4Rα-deficient and IL-4-deficient mice reveal a role for IL-13 in the regulation of Th2 responses. *Current Biology*. **8**, 669–672 (1998).
59. K. Mohrs, A. E. Wakil, N. Killeen, R. M. Locksley, M. Mohrs, A two-step process for cytokine production revealed by IL-4 dual-reporter mice. *Immunity*. **23**, 419–429 (2005).
60. A. Strasser, S. Whittingham, D. L. Vaux, M. L. Bath, J. M. Adams, S. Cory, A. W. Harris, Enforced BCL2 expression in B-lymphoid cells prolongs antibody responses and elicits autoimmune disease. *Proc Natl Acad Sci U S A*. **88**, 8661 (1991).
61. F. M. Ndungu, E. T. Cadman, J. Coulcher, E. Nduati, E. Couper, D. W. MacDonald, D. Ng, J. Langhorne, Functional Memory B Cells and Long-Lived Plasma Cells Are Generated after a Single Plasmodium chabaudi Infection in Mice. *PLoS Pathog*. **5**, e1000690 (2009).
62. G. J. Keitany, K. S. Kim, A. T. Krishnamurty, B. D. Hondowicz, W. O. Hahn, N. Dambrauskas, D. N. Sather, A. M. Vaughan, S. H. I. Kappe, M. Pepper, Blood Stage Malaria Disrupts Humoral Immunity to the Pre-erythrocytic Stage Circumsporozoite Protein. *Cell Rep*. **17**, 3193–3205 (2016).
63. J. J. Taylor, R. J. Martinez, P. J. Titcombe, L. O. Barsness, S. R. Thomas, N. Zhang, S. D. Katzman, M. K. Jenkins, D. L. Mueller, Deletion and anergy of polyclonal B cells specific for ubiquitous membrane-bound self-antigen. *Journal of Experimental Medicine*. **209**, 2065–2077 (2012).

64. J. A. vander Heiden, G. Yaari, M. Uduman, J. N. H. Stern, K. C. O'connor, D. A. Hafler, F. Vigneault, S. H. Kleinstein, pRESTO: a toolkit for processing high-throughput sequencing raw reads of lymphocyte receptor repertoires. *Bioinformatics*. **30**, 1930 (2014).
65. BBTools User Guide - DOE Joint Genome Institute, (available at https://jgi.doe.gov/data-and-tools/software-tools/bbtools/bb-tools-user-guide/).
66. N. T. Gupta, J. A. vander Heiden, M. Uduman, D. Gadala-Maria, G. Yaari, S. H. Kleinstein, Change-O: a toolkit for analyzing large-scale B cell immunoglobulin repertoire sequencing data. *Bioinformatics*. **31**, 3356 (2015).
67. H. Wickham, M. Averick, J. Bryan, W. Chang, L. D', A. Mcgowan, R. François, G. Grolemund, A. Hayes, L. Henry, J. Hester, M. Kuhn, T. Lin Pedersen, E. Miller, S. M. Bache, K. Müller, J. Ooms, D. Robinson, D. P. Seidel, V. Spinu, K. Takahashi, D. Vaughan, C. Wilke, K. Woo, H. Yutani, Welcome to the Tidyverse. *J Open Source Softw*. **4**, 1686 (2019).

Acknowledgements: The authors thank the Pepper lab members - especially Dr. Gretchen Harms Pritchard – as well as the Oberst and Gerner labs for helpful discussions and technical assistance. We also thank Nate Bloom and Dr. Shane Crotty for providing us with tissues from the ΔBPS1 mice, Dr. Chris Allen for the BCL2-Tg mice, and the University of Washington Department of Immunology Flow Cytometry Core and vivarium for their support. Experiment schematics in figures were created with BioRender.com.

Funding: This work was supported by NIH T32 AI206677 and the National Science Foundation Graduate Research Fellowship Program under Grant No. DGE-1762114 (L.S), as well as NIH R01 AI118803, U01 AI42001, and BWF 1016766 (M.P.).

Author contributions: L.S. and M.P. conceived and designed the study. L.S., C.D.T., and L.P. performed experiments. L.S. and C.D.T. analyzed data. B.H. provided technical and conceptual expertise. D.R. and J.C. provided reagents. L.S. and M.P. wrote the manuscript. C.D.T., B.H., L.P., D.R., and J.C. read and edited the manuscript.

Competing interests: M.P. is a member of the NeoLeukin and Vaxart scientific advisory boards.

Data and materials availability: All data are available in the main text or in the supplementary materials.

Supplementary Materials
Figs. S1 to S7
Table S1
Data S1

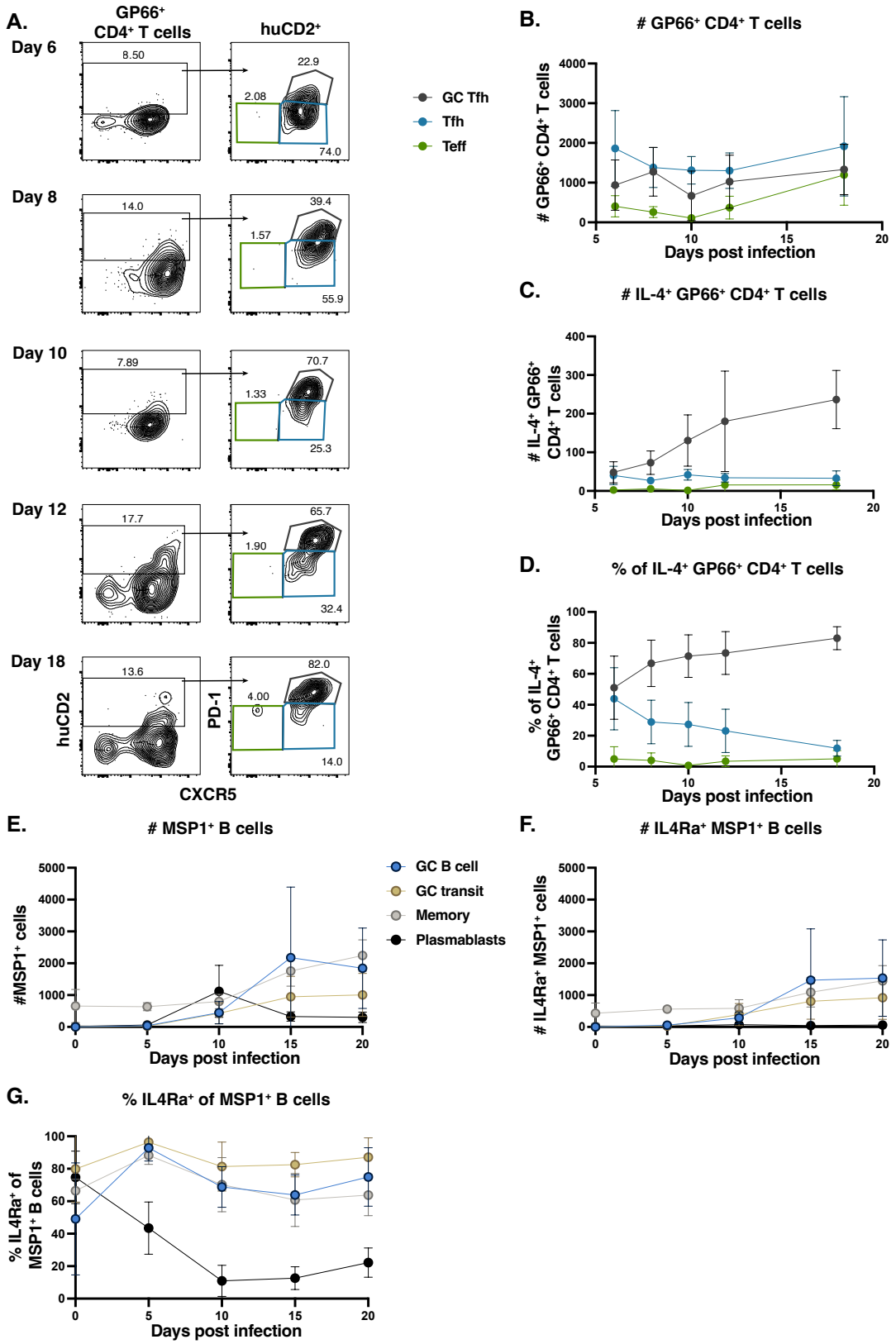

Fig. 1. Kinetics of IL-4 production and IL4Rα expression throughout acute *Plasmodium* infection. KN2$^{+/-}$ mice were infected with blood-stage *P.y*-GP66 and GP66-specific CD4^{+} T cells

were assessed for IL-4 production as measured by surface huCD2 expression at days 6, 8, 10, 12, and 18 post-infection. (**A**) Flow cytometry plots of huCD2$^+$ GP66-specific CD4$^+$ T cells (CD3$^+$CD4$^+$CD8$^-$CD44$^+$GP66$^+$) further gated on GC Tfh (grey; CXCR5$^+$PD-1$^+$), Tfh (blue; CXCR5$^+$PD-1$^-$), and Teff (green; CXCR5$^-$PD-1$^-$) at each time point. (**B**) Number of GP66-specific CD4$^+$ T cells by subset and of (**C**) IL-4-producing (huCD2$^+$) GP66-specific CD4$^+$ T cells by subset. (**D**) Frequency of each T cell subset within the huCD2$^+$ GP66-specific CD4$^+$ T cell population as gated in (A). Data are combined from three independent experiments with 6-8 mice per time point. WT mice were infected with blood-stage *P.y*-GP66 and the MSP1-specific B cell response was analyzed on days 0-20 post-infection. (**E**) Number of MSP1-specific GC B cells (blue; decoy$^-$MSP1$^+$CD138$^-$CD38$^-$GL7$^+$), GC transit B cells (gold; decoy$^-$MSP1$^+$CD138$^-$CD38$^+$GL7$^+$), memory B cells (grey; decoy$^-$MSP1$^+$CD138$^-$CD38$^+$GL7$^-$), and plasmablasts (black; decoy$^-$MSP1$^+$CD38$^-$CD138$^+$) were assessed at each time point indicated. (**F**) Number and (**G**) frequency of IL4Rα-expressing MSP1-specific B cells by subset. Data are combined from three independent experiments with 6 mice per time point.

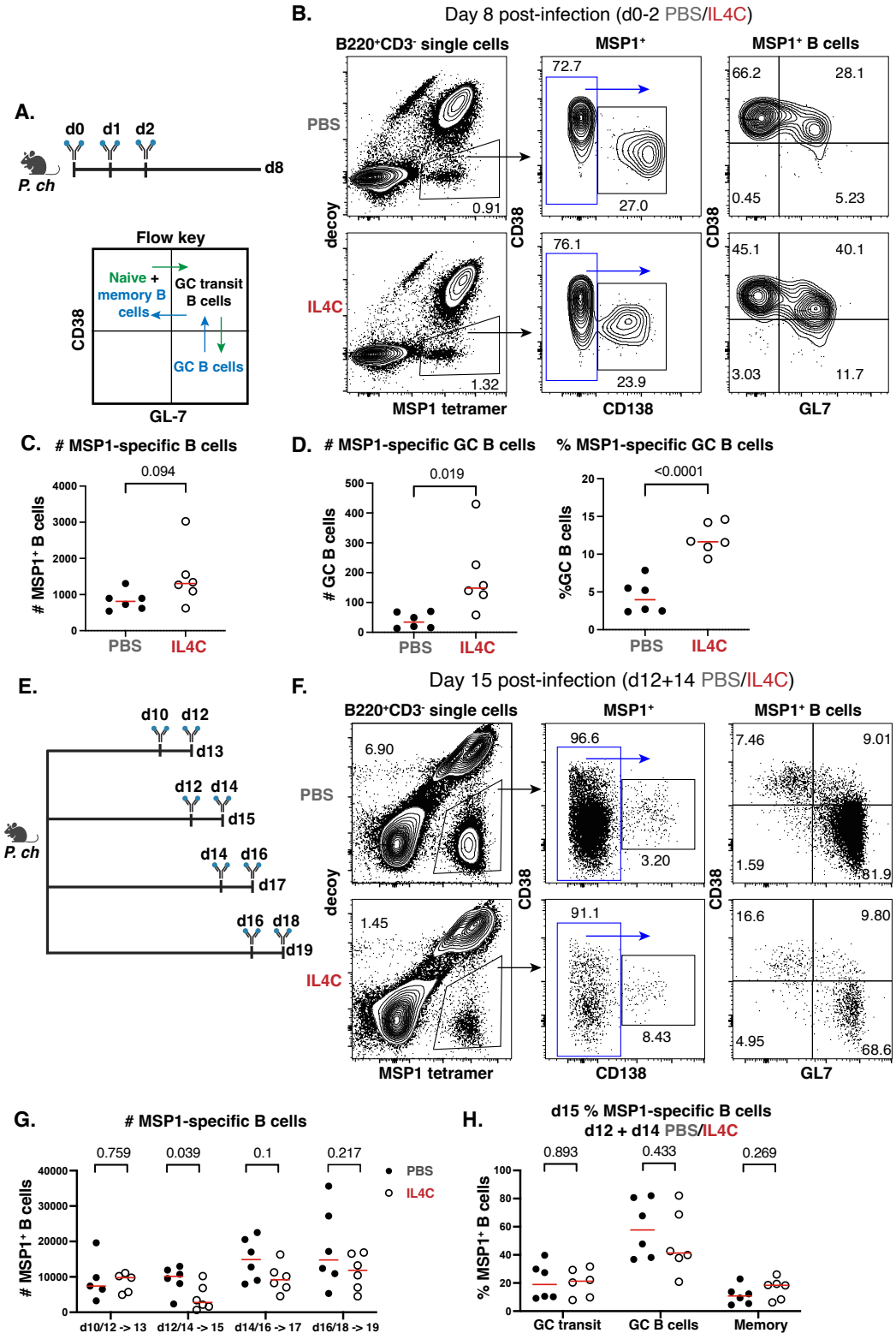

Fig. 2. The effect of IL-4 on the antigen-specific B cell response varies over the course of infection. (**A**) WT mice were infected with *P.ch* and treated with PBS or IL4C on days 0, 1, and

2 post-infection (top). Flow key indicating the identification of naive and memory B cells, GC transit B cells, and GC B cells by CD38 and GL7 expression (bottom). (**B**) Representative flow cytometry plots of MSP1-specific cells (decoy$^-$MSP1$^+$) at 8 days post-infection from mice treated with PBS (top) or IL4C (bottom), with further gating on plasmablasts (CD38$^-$CD138$^+$), memory B cells (CD38$^+$CD138$^-$GL7$^-$), GC transit B cells (CD38$^+$CD138$^-$GL7$^+$), and GC B cells (CD38$^+$CD138$^-$GL7$^+$). (**C**) Total MSP1-specific B cells (decoy$^-$MSP1$^+$CD38$^+$CD138$^-$) in each treatment group at day 8. (**D**) Number (left) and frequency (right) of MSP1-specific GC B cells in each treatment group at day 8. Data are combined from two independent experiments with 6 mice per group. (**E**) WT mice were infected with *P.ch* and treated with IL4C or PBS over two-day windows and MSP1-specific B cell responses were analyzed the following day, as indicated. (**F**) Representative flow cytometry plots from mice treated with PBS (top) or IL4C (bottom) on days 12 and 14 and analyzed on day 15, gating as in (A). (**G**) Number of MSP1-specific B cells at each time point analyzed. (**H**) Frequency of GC transit, GC B cells, and MBCs (CD38$^+$GL7$^-$ CD73$^{and/or}$CD80$^+$) in each treatment group at day 15, following PBS or IL4C treatment on days 12 and 14. Data are combined from two independent experiments with 5-6 mice per group.

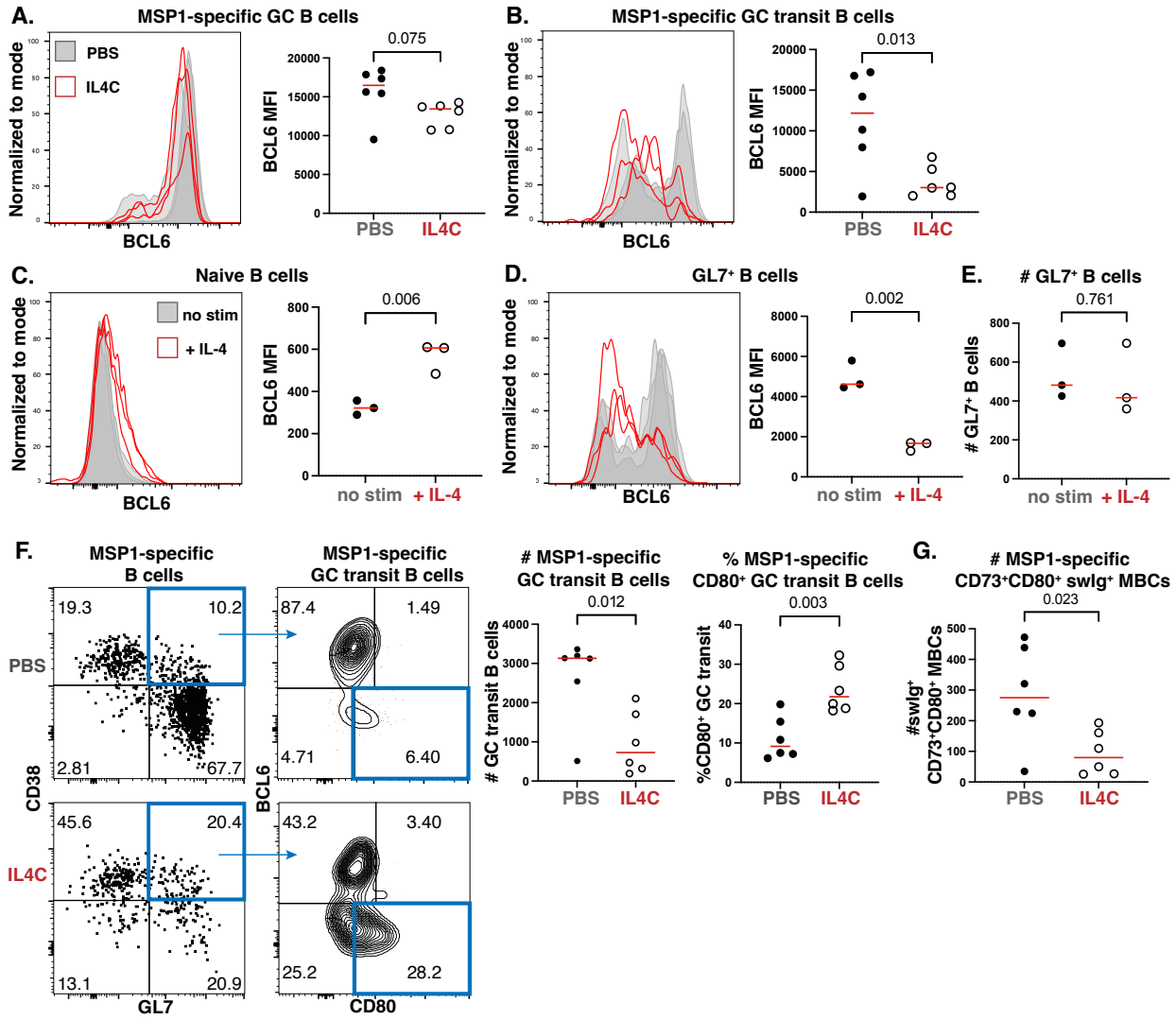

Fig. 3. IL-4 downregulates BCL6 during an ongoing GC. WT mice were infected with *P.ch* and treated with IL4C or PBS on days 12 and 14, and the MSP1-specific B cell response was analyzed on day 15. BCL6 expression in (**A**) GC B cells and (**B**) GC transit B cells at day 15 in mice treated with PBS (grey) or IL4C (red), with representative histograms on the left and quantified median fluorescent intensity (MFI) on the right. B cells were negatively selected from murine splenocytes and cultured with or without 10 ng/mL of recombinant IL-4 for 24h, then stained for flow cytometry. BCL6 expression on (**C**) naive B cells ($B220^{+}CD138^{-}CD38^{+}GL7^{-}IgD^{+}CD73^{-}CD80^{-}$) and (**D**) $GL7^{+}$ B cells ($B220^{+}CD138^{-}IgD^{-}GL7^{+}$). (**E**) Number of $GL7^{+}$ B cells recovered from the 24h culture. Data are combined from three independent experiments, with each symbol representing the average of three technical replicates from each experiment. (**F**) Flow plots (left) depicting GC transit B cells ($CD38^{+}GL7^{+}$) followed by BCL6 by CD80 expression in mice treated with PBS (top) or IL4C (bottom) on days 12 and 14; quantification on the right. (**G**) Number of MSP1-specific $swIg^{+}CD73^{+}CD80^{+}$ MBCs. Data are combined from two independent experiments with 6 mice per group.

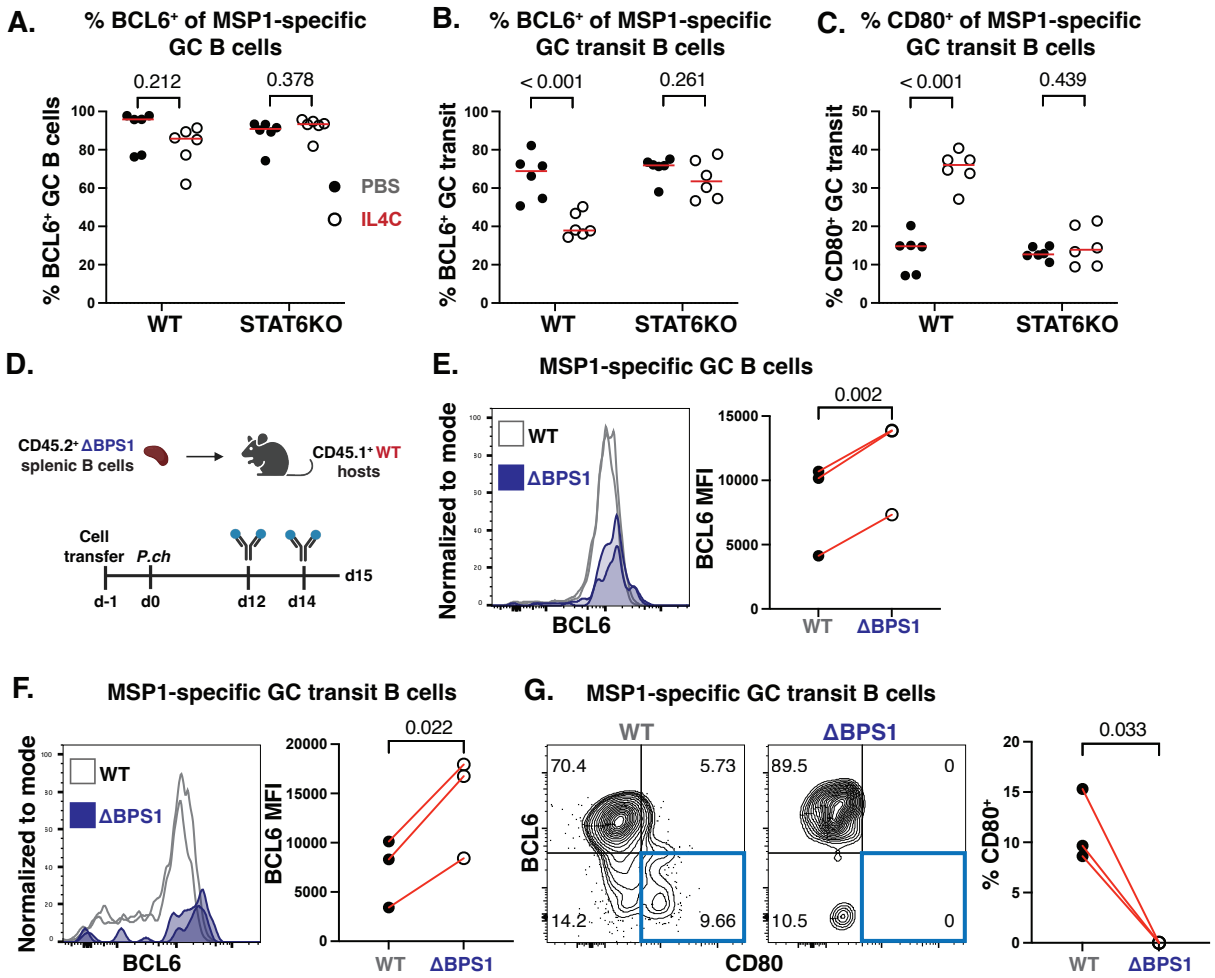

Fig. 4. IL-4 signaling in GL7$^+$ B cells triggers BCL6 negative autoregulation. WT and STAT6KO mice were infected with *P.ch* and treated with IL4C or PBS on days 12 and 14, and the MSP1-specific B cell response was analyzed on day 15. Frequency of MSP1-specific (**A**) GC B cells and (**B**) GC transit B cells expressing BCL6. (**C**) Frequency of MSP1-specific GC transit B cells expressing CD80. Data are combined from two independent experiments with 6 mice per group. (**D**) Splenic B cells were isolated from ΔBPS1 mice and transferred into WT hosts. The mice were infected with *P.ch*, treated with IL4C on days 12 and 14, and the MSP1-specific B cell response was analyzed on day 15. BCL6 expression in WT (grey) and ΔBPS1 (blue) (**E**) GC B cells and (**F**) GC transit B cells on day 15, with representative histograms on the left and quantified MFI on the right. (**G**) Representative flow plots depicting BCL6 by CD80 expression in MSP1-specific GC transit B cells (left) and quantified frequency of CD80$^+$ GC transit B cells (right). Data are from two independent experiments with three mice.

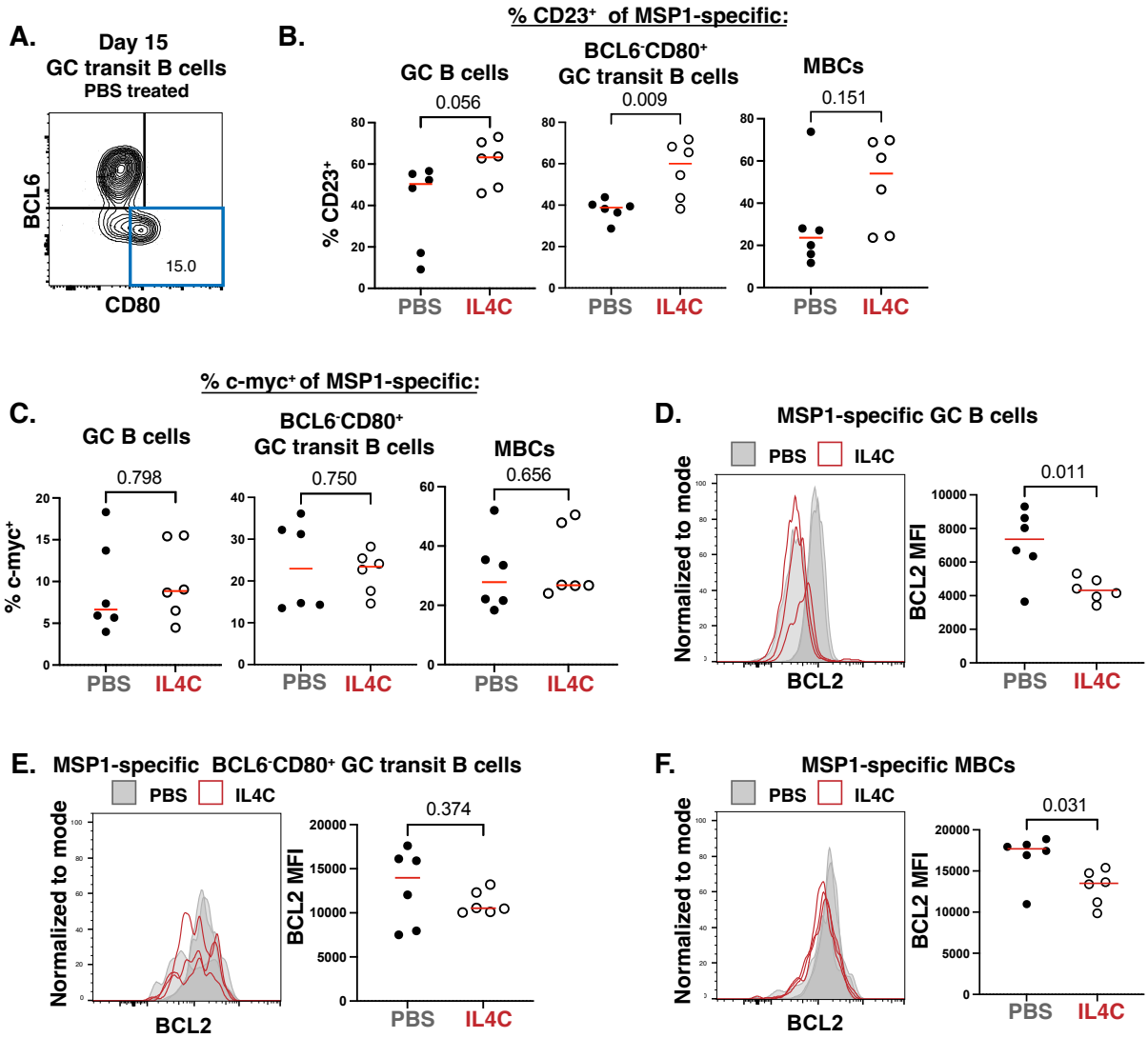

Fig. 5. IL-4 does not promote signals associated with memory B cell survival. WT mice were infected with *P.ch* and treated with IL4C or PBS on days 12 and 14, and the MSP1-specific B cell response was analyzed on day 15. (**A**) Gating strategy for exiting GC B cells, defined as BCL6$^-$CD80$^+$ GC transit B cells. Frequency of (**B**) CD23$^+$ and (**C**) c-myc$^+$ MSP1-specific GC B cells (left), BCL6$^-$CD80$^+$ GC transit B cells (middle), and MBCs (right). Data are combined from three independent experiments with 6 mice per group. BCL2 expression in MSP1-specific (**D**) GC B cells, (**E**) BCL6$^-$CD80$^+$ GC transit B cells, and (**F**) MBCs, with representative histograms on the left and quantified MFI on the right. Data are combined from two independent experiments with 6 mice per group.

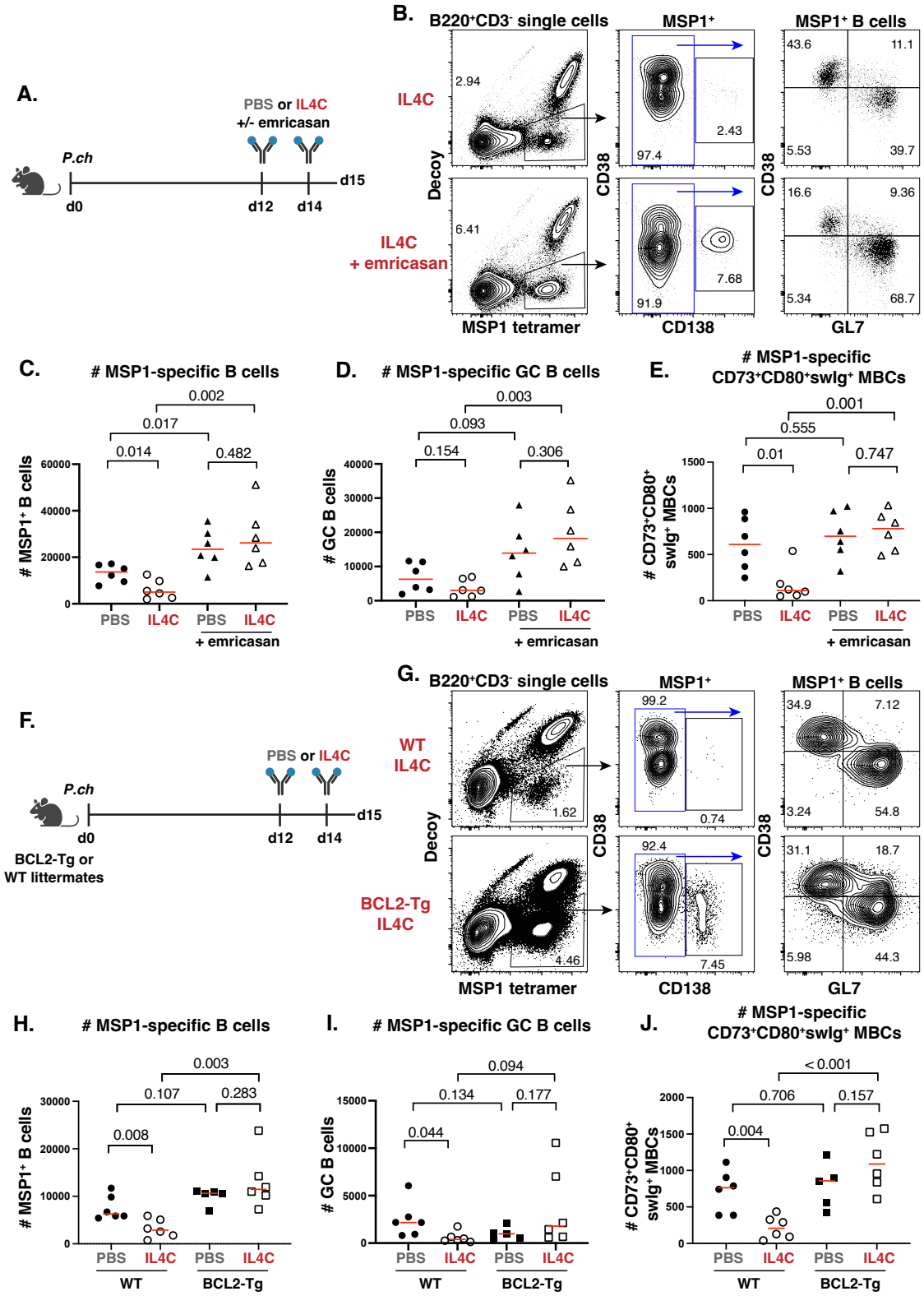

Fig. 6. BCL2 expression is sufficient to rescue B cells from IL-4-mediated death. (**A**) WT mice were infected with *P.ch* and treated with PBS or IL4C both with or without emricasan on days 12

and 14. (**B**) Representative flow plots showing gating on MSP1-specific B cells from mice treated with IL4C (top) or IL4C and emricasan (bottom). Number of MSP1-specific (**C**) total B cells, (**D**) GC B cells, and (**E**) swIg^{+}CD73^{+}CD80^{+} MBCs in each group on day 15 post-infection. Data are combined from three independent experiments with 6 mice per group. (**F**) WT mice and BCL2-Tg littermates were infected with *P.ch* and treated with PBS or IL4C on days 12 and 14 and analyzed on day 15. (**G**) Representative flow plots showing gating on MSP1-specific B cells from WT (top) and BCL2-Tg (bottom) mice treated with IL4C. Number of MSP1-specific (**H**) total B cells, (**I**) GC B cells, and (**J**) swIg^{+} CD73^{+}CD80^{+} MBCs in each group on day 15 post-infection. Data are combined from three independent experiments with 5-6 mice per group.

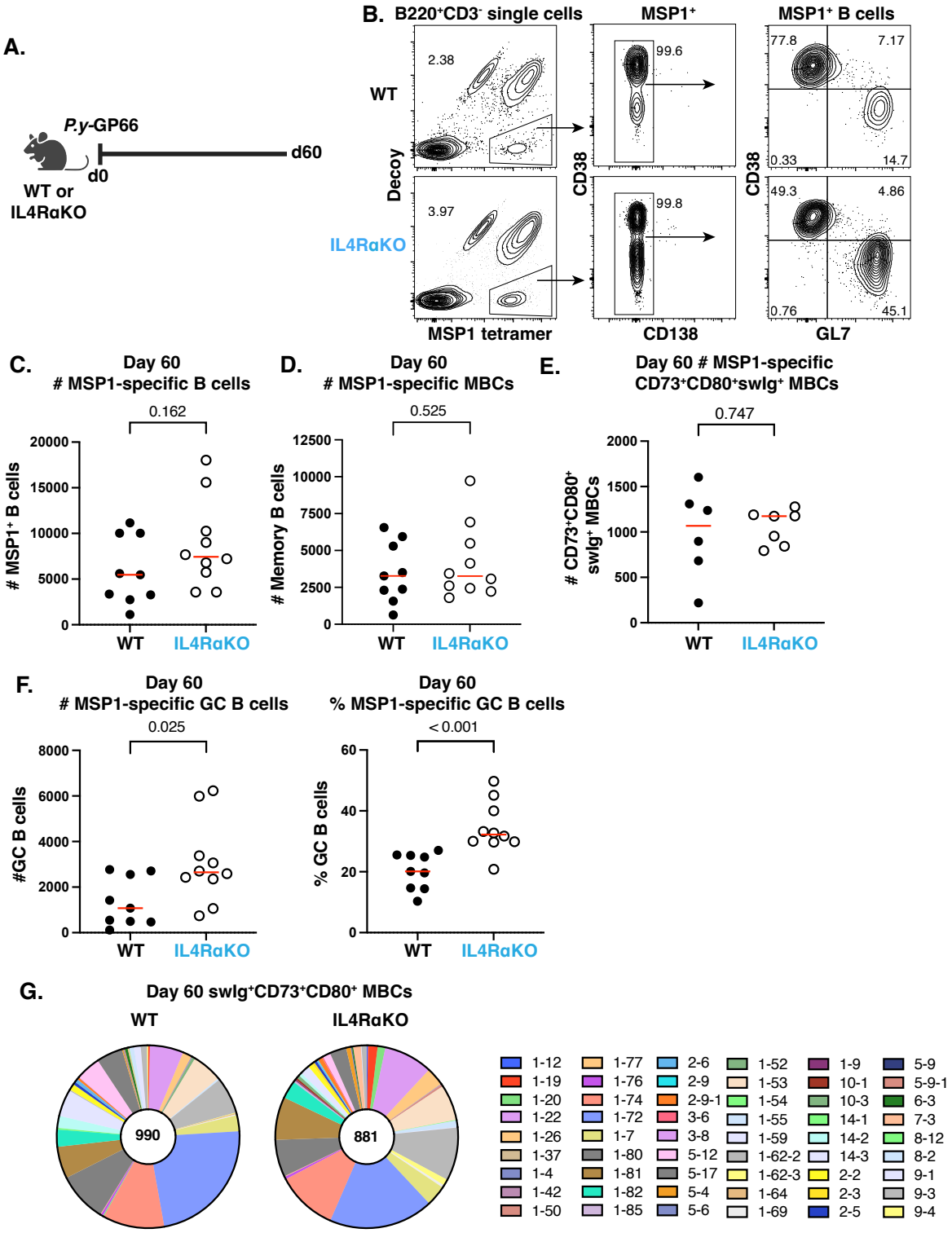

Fig. 7. IL-4 regulates memory B cell selection in the GC. (**A**) WT and IL4RαKO mice were infected with *P.y*-GP66 and the MSP1-specific B cell response was analyzed on day 60. (**B**) Representative flow plots showing gating on MSP1-specific B cells from WT (top) and IL4RαKO (bottom) mice. Number of MSP1-specific (**C**) total B cells, (**D**) total MBCs, and (**E**)

swIg$^+$CD73$^+$CD80$^+$ MBCs. (**F**) Number (left) and frequency (right) of MSP1-specific GC B cells. Data are combined from three independent experiments with 6-10 mice per group. CD73$^+$CD80$^+$ MBCs were sorted from *P.y*-GP66-infected IL4RαKO and WT mice 60 days post-infection. BCRs were cloned and sequenced and swIg$^+$ cells were analyzed for V_H gene usage. (**G**) Pie charts indicating the frequency of V_H gene usage in WT and IL4RαKO swIg$^+$CD73$^+$CD80$^+$ MBCs. Data are combined from two independent experiments with 5-6 mice per group.

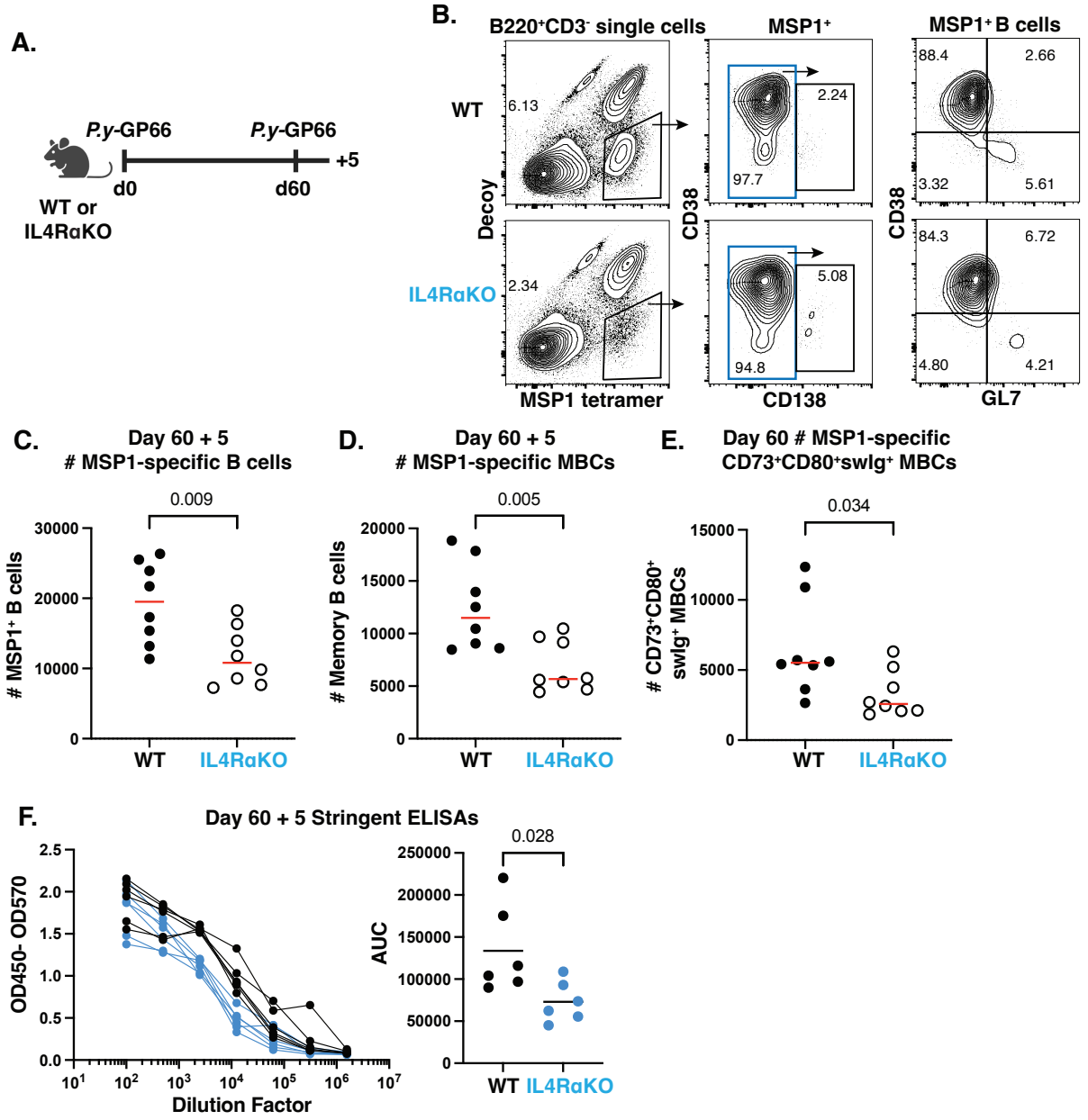

Fig. 8. Memory B cells formed in the absence of IL-4 signaling have a weaker response to re-challenge. (**A**) WT and IL4RαKO mice were re-challenged with *P.y*-GP66 60 days post-infection and the MSP1-specific B cell response was analyzed 5 days post-challenge. (**B**) Representative flow plots showing gating on MSP1-specific B cells from WT (top) and IL4RαKO (bottom) mice. Number of (**C**) total MSP1-specific B cells, (**D**) total MBCs, and (**E**) swIg$^+$CD73$^+$CD80$^+$ MBCs. Data are combined from three independent experiments with 8 mice per group. (**F**) Stringent ELISA dilution curves (left) and AUC (right) for anti-MSP1 IgG in serum collected 5 days post-challenge. Data are combined from two independent experiments with 6 mice per group.